GCAGS JOURNAL
A Publication of the Gulf Coast Association of Geological Societies
www.gcags.org

Carbonate Facies within Siliciclastic Submarine Fan Deposits, Lower Cenozoic Toledo Formation, Southern Belize: Petrography and Provenance

Jason D. Fisher[1,2] and David T. King, Jr.[1]

[1]*Department of Geosciences, Auburn University, 2050 Memorial Coliseum, Auburn, Alabama 36849, U.S.A.*

[2]*George Town, Grand Cayman, KY–1102, Cayman Islands*

ABSTRACT

The Toledo formation in the Belize Basin of southern Belize is an informal Lower Cenozoic (Paleogene) stratigraphic unit, which consists of conglomerate, sandstone, interbedded sandstone and mudstone, and detrital limestone. The Toledo was deposited in a submarine-fan system and is presently well-exposed in southern Belize, particularly along and near the Southern and Mile 14 highways. The present study was undertaken to examine the depositional processes and environments of constituent carbonate facies within this clastic submarine fan system, and to better understand the provenance and tectonic setting of the sandstones. Petrographic analysis of the carbonates reveals that the skeletal grains represent an Early Cenozoic open-marine assemblage of crinoids and echinoids that is combined with a restricted marine assemblage of gastropods, foraminifera, and algae. Non-skeletal grains vary widely in abundance between carbonate beds, and generally consist of oöids, peloids, and terrigenous grains. The carbonate facies are interpreted to be slope deposits. Lithic analysis of the coeval Toledo sandstones indicates an average composition of 34% quartz, 2% feldspar, and 64% lithic fragments; thus all samples are classified as lithic arenites. These lithic fragments include limestone clasts, and a variety of igneous rock fragments. Diagenesis of both carbonates and sandstones includes initial cementation (and thus reduction of existing pore spaces), followed by compaction and silicification. Ternary plots of framework mineralogy indicate derivation from a recycled orogen, which may be related to the Early Cenozoic collision of the North America and Caribbean tectonic plates.

INTRODUCTION

The informal Lower Cenozoic (Paleogene) Toledo formation, crops out in a wide area within the Belize Basin (south of the Maya Mountains of Belize), where the formation is approximately 3000 m or more in thickness. Deposition of the Toledo started during Paleogene when the Belize basin was experiencing a shift in sedimentation from a carbonate-dominated basin (i.e., the Coban and Campur formations) to a clastic dominated basin receiving submarine deposits of the Toledo formation (Fisher and King, 2016).

The Belize Basin is a Late Jurassic to Paleogene feature located south of the Maya Mountains in southern Belize (Fig. 1). This basin is the eastward extension of the Chapayal Basin (or the Southern Petén Basin) of Guatemala (Vinson, 1962; Bryson, 1975; Donnelly et al., 1990; Kim et al., 2011), and is both an onshore and offshore feature of southern Belize geology. The basin is bounded on the north by the Southern Boundary fault of southern Belize, and just south of the southern limit of the basin is the Polochic fault system, a left-lateral strike-slip fault system, related to the collision of the North American and Caribbean plates. The Cenozoic stratigraphic section of the Belize basin crops out over a wide area in the Toledo District of southern Belize. Particularly along the northeast-trending section of the Southern highway (i.e., the highway follows along approximate depositional dip in the eastern part of the Belize Basin), Cenozoic strata of the Toledo formation crop out as far south as the village of Dump (Fig. 1). Also, on the newly constructed Mile 14 highway, westward from Dump toward the Guatemalan border, there is a well-exposed, approximate-strike section of the clastic Toledo formation. The Mile 14 highway section represents the middle part of the Belize Basin. In the whole of the Belize Basin, the Toledo attains maximum thicknesses of up to approximately 3000 m (as observed in exploratory wells; Purdy et al., 2003), however in outcrop 100 to 200 m of section, mainly the upper part of the Toledo formation, are well-exposed.

The Toledo formation is composed of sandstone, sandstone interbedded with mudstone, conglomerate, and carbonate (detrital limestone). Sandstone is the dominant lithology throughout the formation, and these sandstones are mineralogically and textural-

Manuscript received January 14, 2019; revised manuscript received February 27, 2019; manuscript accepted June 5, 2019.

GCAGS Journal, v. 8 (2019), p. 153–169.
DOI: pending

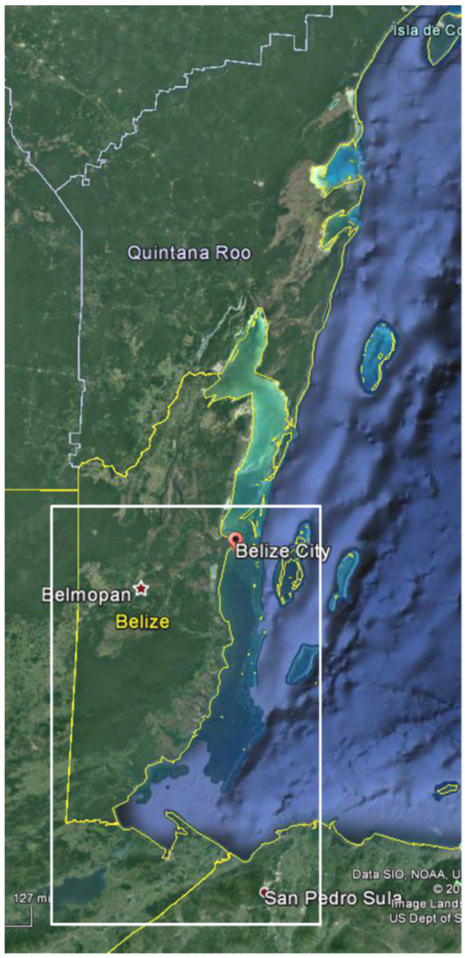
Quintana Roo
Belize City
Belmopan
Belize
San Pedro Sula

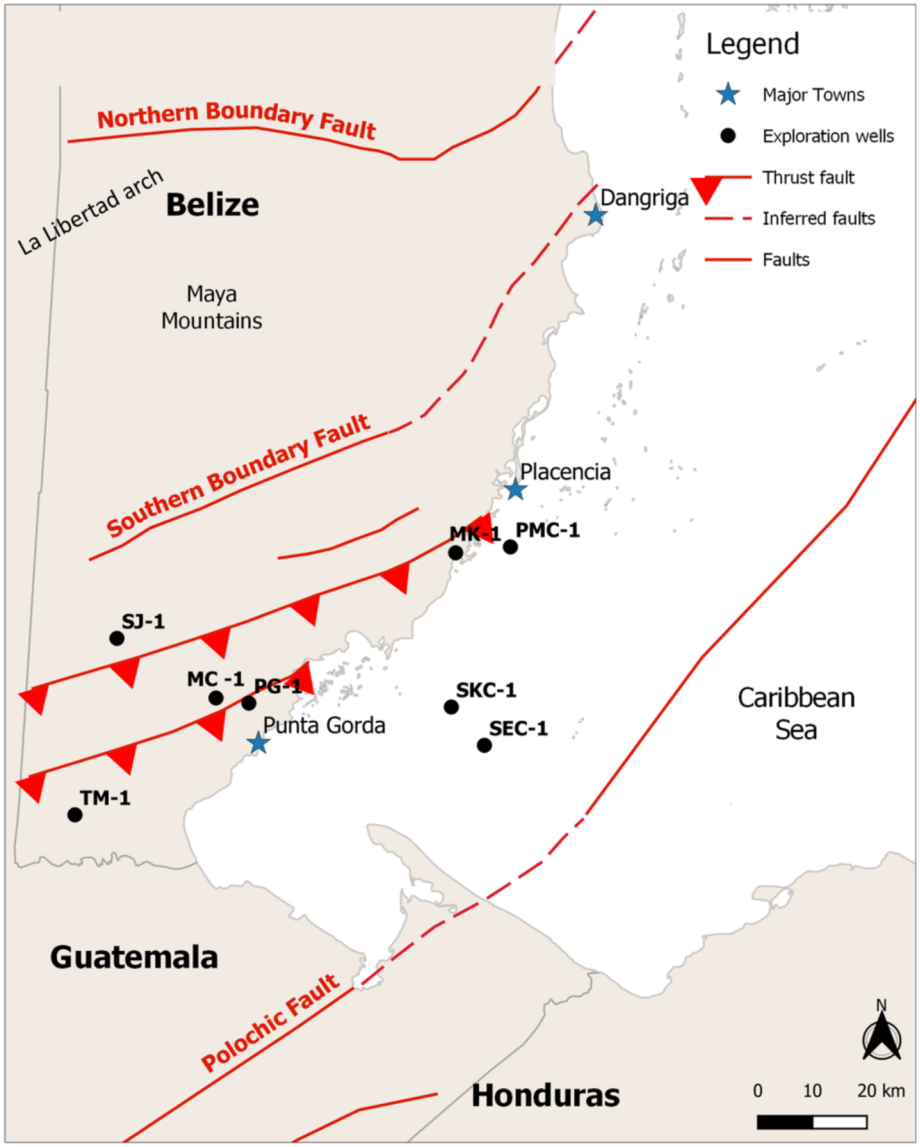
Legend
Major Towns
Exploration wells
Thrust fault
Inferred faults
Faults
Northern Boundary Fault
La Libertad arch
Belize
Maya Mountains
Dangriga
Southern Boundary Fault
Placencia
MK-1
PMC-1
SJ-1
MC -1
PG-1
Punta Gorda
SKC-1
SEC-1
TM-1
Caribbean Sea
Guatemala
Polochic Fault
Honduras
N
0 10 20 km

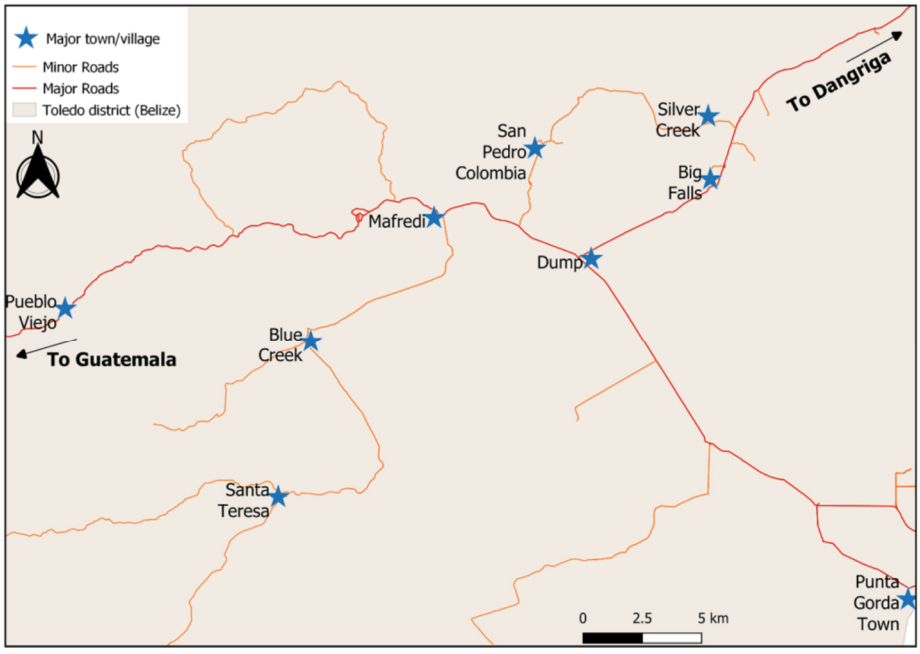
Major town/village
Minor Roads
Major Roads
Toledo district (Belize)
N
To Dangriga
Silver Creek
San Pedro Colombia
Big Falls
Mafredi
Dump
Pueblo Viejo
To Guatemala
Blue Creek
Santa Teresa
Punta Gorda Town
0 2.5 5 km

(FACING PAGE) Figure 1. Location maps. Upper left—Google Earth® image of Belize area with white box showing area of map in upper right. Upper right—Simplified structural map of central and southern Belize showing key faults, major towns, and locations of exploratory wells drilled (modified after Purdy et al., 2003). The Belize Basin lies between the Southern Boundary fault of southern Belize and the Polochic fault of northern Guatemala. Lower part—Sketch map of southern Belize showing highways, roads, and key towns. The study area's field sites follow the southern highway to Dump and from Dump to a few km west of Pueblo Viajo. Geographic information system (GIS) base maps for this figure were retrieved from diva-gis.org.

ly immature (Fisher and King, 2016). The sandstone has been described as poorly sorted calcarenites containing igneous rock fragments, limestone grains, and chert particles (Vinson, 1962; Fisher and King, 2016). Carbonates (detrital limestones) are volumetrically minor constituents of the Toledo formation and these limestones occur in two main facies: carbonate breccia, and wackestone-packstone (Fisher and King, 2016).

This study presents the results of textural and mineralogical analysis from carbonate and clastic samples collected during the 2016 field session. The main objectives of this study are: (1) describe and interpret the petrography of Toledo limestone facies within the Toledo formation; (2) describe and interpret the petrography of Toledo sandstone facies and their economic (reservoir) potential; and (3) interpret the tectonic setting of Toledo submarine-fan facies based on the limestone components and the petrography of sandstones.

MATERIALS AND METHODS

In the present study, we examined exposures of the Toledo formation along the Southern Highway in the Toledo District as far south as the village of Dump, and then westward along the newly built Mile 14 Highway from Dump to a few kilometers east of the Guatemalan border (Fig. 1). Representative sandstone and carbonate samples were taken at a total of 38 localities (see locality information in Fisher and King [2015]). Conventional petrographic analysis was conducted on 38 thin sections, including compositional point counts, using JMicroVision (2018). The JMicroVision software was developed for visualization and analysis of petrographic images. Tools within the software allow for granulometric analysis and computerized point-counting. This provides an alternative to conventional estimates of modal composition and is carried out on thin-section photomicrographs. Four to six photomicrographs were made for each thin section, and a mineralogical determination and count of 300 points for each thin section were completed in each instance. For sandstone, the framework detrital composition was based on methods of Dickinson (1985) (Table 1) and these data were plotted on ternary diagrams of Dickinson and Suczek (1979), which feature three plate tectonic provenances.

For the carbonates, we used the following terms for relative frequencies of allochemical grains (allochems) identified in the samples—very rare, <2%; rare, 2–5%; sparse, 5–10%; common, 10–30%; very common, 30-50%; and abundant, >50%. These frequencies represent the percentage of total grains unless otherwise stated. The allochems are divided into skeletal and non-skeletal grains.

Thirteen compositional classes were identified for Toledo sandstones and fourteen were identified for Toledo carbonates (Tables 2 and 3). The default uniform random grid was utilized. The results of point counting are presented herein as volume percentage unless otherwise stated.

Plate tectonics plays an important role in determining the characteristics of detrital grains of sandstones (Dickinson and Suczek, 1979; Dickinson et al, 1983; Bhatia, 1983; Roster and Korsch, 1986). The ratio of framework grains (quartz, feldspar, and lithic fragments) provides important evidence of the lithology of the source rocks. The method used follows the Dickinson (1985) scheme, briefly described below.

Dickinson (1985) described sandstones based on their detrital framework grain composition, which is largely controlled by the tectonic setting of their provenance. The major provenance types related to continental sources identified are stable cratons, basement uplifts, magmatic arcs, and recycled orogens. Detailed descriptions of these provenance types can be found in Dickinson and Suczek (1979) and Dickinson (1985).

Based on Dickinson (1985), grain types are classified as monocrystalline quartz (Qm), polycrystalline quartz (Qp), total feldspar (F), volcanic/metavolcanic lithic fragments (Lv), and sedimentary/metasedimentary lithic fragments (Ls) (Table 1). Detrital modes are recalculated to 100% as the sum of the above-mentioned grain types (Table 3). Carbonate grains (Lc) are not recalculated with other lithic fragments (Lv and Ls) because of the geochemical response during weathering and diagenesis, coupled with the potential for confusion between extra- (i.e., reworked) and intra-basinal carbonate grains (intraclasts, bioclasts, oöliths, peloids).

CARBONATE PETROGRAPHY

Skeletal Grains

Skeletal grains, which account for 2 to 24% by volume of Toledo carbonate rock, consist of fragments of invertebrate body fossils and algal fossil debris (Table 2). The skeletal grains generally lack evidence of transport and abrasion, i.e., little or no rounding. This suggests that initial deposition may have taken place in relatively low energy environments. Some skeletal grains are classified as generic bioclasts because of the loss of taxonomically distinguishing features because of diagenesis.

Based on the nature of constituent skeletal grains, we can define two assemblages: open-marine and restricted-marine. Figures 2 and 3 are photomicrographs that show examples of these grains, and some non-skeletal grains as well. The open-marine assemblage is very rare and consists of echinoids and corals, which comprise only about 1% by volume of all skeletal grains. Unlike the more common restricted-marine assemblage, echinoids and corals would have required normal, open-marine conditions for life.

In general, restricted marine assemblages are known to be tolerant of adverse environmental conditions, namely variations in salinity. In the Toledo, this assemblage is common, and consists of —in order of decreasing abundance—red algae, gastropods (mollusks), and foraminifera (in total, these grains range from 1 to 19% by volume of skeletal grains).

Non-Skeletal Grains

Non-skeletal grains, which make up between 62 to 97% by volume of Toledo carbonate rock, consist of carbonate lithic fragments, peloids, and terrigenous grains (Figs. 2 and 3). Lithic fragments, which range from 52 to 80% by volume, make up the majority of the non-skeletal grains within Toledo carbonate samples. Lithic fragments are dominated by reworked limestone clasts, which are typically micritized and contain skeletal grains of various sizes within them. Igneous/metamorphic lithic fragments are rare to common and quartz and feldspar mineral grains are rare to sparse.

Table 1. Grain-type classification used in the present paper (based on Dickinson, 1985).

Quartzose grains (Q = Qm + Qp)

Q = Total quartzose grains

Qm = monocrystalline quartz
Qp = polycrystalline quartz

Feldspar grains (F)

Unstable lithic fragments (L = Lv + Ls)
L = total unstable lithic fragments
Lv = volcanic/metavolanic lithic fragments

Total lithic fragments (Lt = L + Qp)
Lc = extrabasinal detrital limestone (not included in L or Lt)

Table 2. Summary of point-count results (as percents) for carbonate samples from the Toledo formation. In the lower dataset, point-count classes are recalculated as a total percentage, i.e., not including matrix and cement. *, calculated as total percentage including matrix and cement; and **, calculated as total percentage excluding matrix and cement.

Sample	FTD14A	FTD28A	FTD41A	WP438
Point-count classes (%)				
*Skeletal grains**				
Bioclasts	0.80	3.17	1.67	3.00
Mollusks	0.00	0.67	3.17	1.00
Echinoids	0.00	0.33	0.00	0.00
Foraminiferae (planktic)	0.20	0.00	0.00	0.00
Foraminiferae (unidentified)	0.20	0.17	0.67	0.33
Red algae	0.40	11.50	6.33	8.00
*Non-skeletal grains**				
Oöids	8.40	0.00	0.00	0.00
Peloids	0.00	17.67	5.00	5.00
Quartz	3.90	0.00	0.00	1.33
Feldspar	0.30	0.00	0.00	0.00
Lithics	51.20	23.33	53.83	52.67
Matrix	1.40	3.17	0.50	0.00
Cement	33.20	40.00	28.83	28.67
*Skeletal grains***				
Bioclasts	1.22	4.84	2.55	4.59
Mollusks (incl. rudists)	0.00	1.02	4.84	1.53
Echinoids	0.00	0.51	0.00	0.00
Foraminiferae (planktic)	0.31	0.00	0.00	0.00
Foraminiferae (unidentified)	0.31	0.25	1.02	0.51
Red algae	0.61	17.58	9.68	12.23
	2.45	24.21	18.09	18.86
*Non-skeletal grains***				
Oöid	12.84	0.00	0.00	0.00
Peloid	0.00	27.01	7.65	7.65
Quartz	5.96	0.00	0.00	2.04
Feldspar	0.46	0.00	0.00	0.00
Lithics	78.28	35.68	82.32	80.53

Table 3. Framework components obtained from point-count data of sample numbers listed above columns. All values in this table are volume percents.

Sample Number	06A	07B	10	12A	13	16A	18A
Total quartz (% framework)	9.67	9.00	13.95	16.67	7.67	8.67	16.33
Total monocrystalline quartz (% framework)	8.00	5.33	10.30	12.67	5.67	7.33	12.00
Total polycrystalline quartz (% framework)	1.67	3.67	3.65	4.00	2.00	1.33	4.33
Total feldspar (% framework)	0.33	0.00	0.00	2.00	2.33	1.33	0.33
Total carbonate lithics (% framework)	22.67	13.67	0.00	1.33	10.00	8.00	13.00
Total igneous grains (% framework)	29.00	35.00	29.24	28.00	24.67	30.00	13.67
Total unidentified lithics (% framework)	12.67	15.67	22.92	22.33	24.33	16.00	6.33
Total fossil (% framework)	2.33	2.67	0.00	0.00	0.00	0.00	0.33
Total organic matter (% framework)	0.00	0.00	0.00	0.00	0.00	0.00	6.67
Total mica (% framework)	0.00	0.00	0.33	0.67	0.00	0.33	0.67
Total matrix (% framework)	2.00	2.67	10.96	17.67	17.67	13.67	13.00
Total cement (% framework)	21.33	21.33	22.59	11.33	12.33	22.00	29.67
Total pore (% framework)	0.00	0.00	0.00	0.00	1.00	0.00	0.00
Q—total quartz (Dickinson) (% total QFL)	29.00	20.46	32.31	35.71	22.12	21.67	53.85
F—feldspathic components (Dickinson) (% total QFL)	1.00	0.00	0.00	4.29	6.73	3.33	1.10
L—lithic components (Dickinson) (% total QFL)	87.00	79.55	67.69	60.00	71.15	75.00	45.05
Qm—monocrystalline quartz (Dickinson) (% total QmFL)	20.51	12.10	23.85	27.14	16.35	18.33	39.56
F—feldspathic components (Dickinson) (% total QmFL)	0.85	0.00	0.00	4.29	6.73	3.33	1.10
Lt—lithic components (Dickinson) (% total QmFL)	78.63	87.90	76.15	68.57	76.92	78.33	59.34

Sample Number	24A	32.2	34A	36A	42A	46A	50B
Total quartz (% framework)	8.33	21.67	7.33	5.33	16.00	11.67	21.67
Total monocrystalline quartz (% framework)	7.00	16.67	5.33	4.00	14.00	10.00	19.67
Total polycrystalline quartz (% framework)	1.33	5.00	2.00	1.33	2.00	1.67	2.00
Total feldspar (% framework)	0.33	1.00	2.33	2.33	1.00	0.00	0.00
Total carbonate lithics (% framework)	26.67	10.00	26.33	30.00	18.33	27.00	25.00
Total igneous grains (% framework)	19.00	21.67	19.33	26.00	16.33	23.33	24.33
Total unidentified lithics (% framework)	8.33	15.00	3.00	3.67	1.67	0.00	0.67
Total fossil (% framework)	0.00	0.00	0.33	0.67	0.33	0.33	1.67
Total organic matter (% framework)	0.00	0.00	0.00	0.00	4.33	0.00	0.00
Total mica (% framework)	0.00	1.00	0.00	0.00	0.00	0.00	0.33
Total matrix (% framework)	6.67	7.67	5.67	0.00	11.00	0.33	3.67
Total cement (% framework)	30.67	22.00	35.67	31.00	31.00	37.33	22.67
Total pore (% framework)	0.00	0.00	0.00	1.00	0.00	0.00	0.00
Q—total quartz (Dickinson) (% total QFL)	30.12	48.87	25.29	15.84	50.94	33.33	47.10
F—feldspathic components (Dickinson) (% total QFL)	1.20	2.26	8.05	6.93	2.83	0.00	0.00
L—lithic components (Dickinson) (% total QFL)	68.67	48.87	66.67	77.23	46.23	66.67	52.90
Qm—monocrystalline quartz (Dickinson) (% total QmFL)	25.30	37.59	18.39	11.88	39.62	28.57	42.75
F—feldspathic components (Dickinson) (% total QmFL)	1.20	2.26	8.05	6.93	2.83	0.00	0.00
Lt—lithic components (Dickinson) (% total QmFL)	73.49	60.15	73.56	81.19	57.55	71.43	57.25

Table 3, continued.

Sample Number	51A	58A	59A	62A	72A	74A	75A
Total quartz (% framework)	7.67	23.33	21.33	11.00	12.00	9.33	12.67
Total monocrystalline quartz (% framework)	6.33	17.67	16.00	9.33	10.00	7.67	8.33
Total polycrystalline quartz (% framework)	1.33	5.67	5.33	1.67	2.00	1.67	4.33
Total feldspar (% framework)	0.33	0.33	0.33	0.33	0.67	1.00	0.33
Total carbonate lithics (% framework)	29.67	20.67	20.67	29.00	21.00	19.33	20.33
Total igneous grains (% framework)	24.00	19.33	27.67	16.33	22.67	19.67	26.00
Total unidentified lithics (% framework)	0.67	0.33	1.33	0.67	3.00	1.33	0.67
Total fossil (% framework)	2.67	2.00	4.67	5.33	0.33	1.00	0.33
Total organic matter (% framework)	0.00	0.00	0.00	0.00	0.33	0.00	0.00
Total mica (% framework)	0.00	0.00	0.00	0.00	0.00	0.33	0.00
Total matrix (% framework)	1.33	1.67	4.00	3.00	4.33	2.00	1.33
Total cement (% framework)	33.67	32.33	20.00	34.33	35.67	46.00	38.33
Total pore (% framework)	0.00	0.00	0.00	0.00	0.00	0.00	0.00
Q—total quartz (Dickinson) (% total QFL)	23.96	54.26	43.24	39.76	33.96	31.11	32.48
F—feldspathic components (Dickinson) (% total QFL)	1.04	0.78	0.68	1.20	1.89	3.33	0.85
L—lithic components (Dickinson) (% total QFL)	75.00	44.96	56.08	59.04	64.15	65.56	66.67
Qm—monocrystalline quartz (Dickinson) (% total QmFL)	19.79	41.09	32.43	33.73	28.30	25.56	21.37
F—feldspathic components (Dickinson) (% total QmFL)	1.04	0.78	0.68	1.20	1.89	3.33	0.85
Lt—lithic components (Dickinson) (% total QmFL)	79.17	58.14	66.89	65.06	69.81	71.11	77.78

Sample Number	76A	77c	78A	79D	79E	80A
Total quartz (% framework)	15.00	15.67	9.33	3.67	12.67	23.33
Total monocrystalline quartz (% framework)	13.33	13.33	7.00	2.67	10.33	17.67
Total polycrystalline quartz (% framework)	1.67	2.33	2.33	1.00	2.33	5.67
Total feldspar (% framework)	1.00	0.33	0.00	0.00	0.67	1.33
Total carbonate lithics (% framework)	26.00	27.00	28.67	43.00	28.00	19.00
Total igneous grains (% framework)	29.00	19.33	18.33	16.00	30.33	25.67
Total unidentified lithics (% framework)	0.67	1.00	0.00	0.00	0.00	0.33
Total fossil (% framework)	0.00	0.67	1.67	4.00	1.67	0.00
Total organic matter (% framework)	0.00	0.00	0.67	0.00	0.00	1.67
Total mica (% framework)	0.33	0.67	0.00	0.00	0.00	1.00
Total matrix (% framework)	1.67	0.67	0.00	0.00	3.33	2.67
Total cement (% framework)	26.33	34.67	41.33	33.33	23.00	25.00
Total pore (% framework)	0.00	0.00	0.00	0.00	0.33	0.00
Q—total quartz (Dickinson) (% total QFL)	48.57	44.34	33.73	18.64	28.79	46.36
F—feldspathic components (Dickinson) (% total QFL)	1.71	0.94	0.00	0.00	1.52	2.65
L—lithic components (Dickinson) (% total QFL)	49.71	54.72	66.27	81.36	69.70	50.99
Qm—monocrystalline quartz (Dickinson) (% total QmFL)	22.86	37.74	25.30	13.56	23.48	35.10
F—feldspathic components (Dickinson) (% total QmFL)	1.71	0.94	0.00	0.00	1.52	2.65
Lt—lithic components (Dickinson) (% total QmFL)	75.43	61.32	74.70	86.44	75.00	62.25

Table 3, continued.

Sample Number	WP395	WP396	WP398	WP401	WP405	WP427	WP428
Total quartz (% framework)	13.67	14.33	8.00	15.00	18.33	21.33	11.33
Total monocrystalline quartz (% framework)	11.33	11.67	4.67	12.33	15.33	17.33	9.33
Total polycrystalline quartz (% framework)	2.33	2.67	3.33	2.67	3.00	4.00	2.00
Total feldspar (% framework)	1.00	1.00	2.33	0.00	1.00	0.33	0.00
Total carbonate lithics (% framework)	16.00	28.67	19.67	26.67	7.00	23.33	43.00
Total igneous grains (% framework)	37.67	23.00	40.00	23.67	49.00	25.67	25.00
Total unidentified lithics (% framework)	2.00	3.00	1.67	2.67	4.00	2.67	2.00
Total fossil (% framework)	2.00	0.00	0.00	0.67	0.00	0.33	3.00
Total organic matter (% framework)	0.00	0.00	3.33	0.33	0.00	0.00	0.00
Total mica (% framework)	0.00	0.00	0.00	0.00	0.00	0.00	0.00
Total matrix (% framework)	0.33	3.33	0.67	0.00	1.00	3.33	0.67
Total cement (% framework)	27.33	26.67	24.33	31.00	19.67	23.00	15.00
Total pore (% framework)	0.00	0.00	0.00	0.00	0.00	0.00	0.00
Q—total quartz (Dickinson) (% total QFL)	26.11	37.39	15.89	38.79	26.83	45.07	31.19
F—feldspathic components (Dickinson) (% total QFL)	1.91	2.61	4.64	0.00	1.46	0.70	0.00
L—lithic components (Dickinson) (% total QFL)	71.97	60.00	79.47	61.21	71.71	54.23	68.81
Qm—monocrystalline quartz (Dickinson) (% total QmFL)	21.66	30.43	9.27	31.90	22.44	36.62	25.69
F—feldspathic components (Dickinson) (% total QmFL)	1.91	2.61	4.64	0.00	1.46	0.70	0.00
Lt—lithic components (Dickinson) (% total QmFL)	76.43	66.96	86.09	68.10	76.10	62.68	74.31

Peloids are nearly round carbonate grains, which are typically composed entirely of micrite and are generally lacking in any discernible internal structure. As a volumetric constituent, peloids are generally sparse to common (Table 3). In some instances, it is difficult to distinguish reworked very small limestone clasts from peloids, especially if the clasts are well rounded.

Carbonate Depositional Setting

Based on the locality of the study area and the facies described, the depositional environment for the Toledo carbonates is within the "T Carbonate factory" as described by Schlager (2005) (Fig. 4). The "T" represents tropical or "top of the water column" and is limited to the tropical zone between 30°N and 30°S. Carbonates of the Toledo formation are consistent with two of Schlager's facies, namely facies 2 (deep shelf) and facies 4 (slope; Fig. 4). The carbonate samples from the Toledo formation are dominated by reworked lithic grains of various sizes. The skeletal grains are dominated by shallow-water benthic taxa particularly algae, mollusks, and foraminifera (both benthic and planktic).

Schlager's facies 2 was deposited below fair-weather wave base, but within reach of storm waves in close proximity to the euphotic zone. This facies is characterized by skeletal wackestone and some grainstone, bioturbation, and the presence of shelly fauna indicating normal marine conditions in the adjacent biogenic source area. In the study area, facies 2 wackestone-packstone beds are generally tabular, tan to buff, laterally extensive, and range in thickness from 0.5 m to 1 m. These carbonate beds are commonly associated with interbedded, 0.05 to 0.40 m thick sandstones and mudstones. Figures 5A and 5B shows typical outcrops of beds of the Toledo equivalent of Schlager's facies 2 in the study area.

Schlager's facies 4, which was deposited on a sedimentary slope, represents a platform margin and consists of predominantly of reworked platform admixtures with highly variable grain sizes. This breccia facies' taxa consists of mostly redeposited shallow-water benthic taxa and some deepwater benthics and plankton. Texturally, the rock is a breccia that is a very poorly sorted mixture of many rock types, including carbonates and crystalline clasts (Figs. 5C and 5D).

SANDSTONE PETROLOGY

Sandstones are the dominant lithology found throughout the various submarine-fan facies of the Toledo formation (Figs. 6 and 7). Figure 6 shows example photomicrographs showing constituent grains (labeled). Vinson's (1962) original analysis of the Toledo sandstones described them as poorly sorted, calcarenites containing igneous lithic fragments, limestone grains, and chert. However, in the work by Fisher and King (2016) and in the present study, petrographic analysis clearly shows that the Toledo sandstones are lithic arenites.

Texturally, the Toledo sandstones are poorly sorted, with angular to rounded grains. The sandstones are mainly grain-supported and generally contain less than 15% matrix by volume. Specifically, they are best described as immature to submature arenites (in the classification of Boggs [2012]). Most intergranular pore spaces are filled with carbonate cement.

Compositionally, the Toledo sandstones are dominated by lithic fragments, and the lesser constituents by volume are quartz and rare feldspar grains (Table 3). The lithic fragments are dominated by carbonate grains, particularly limestone and skeletal fragments, and the lesser constituents by volume are igneous and unidentified lithics. The limestone grains are fossiliferous to unfossiliferous and the grains are typically micritized, as noted previously. The fossil fragments include corals, algae, and forami-

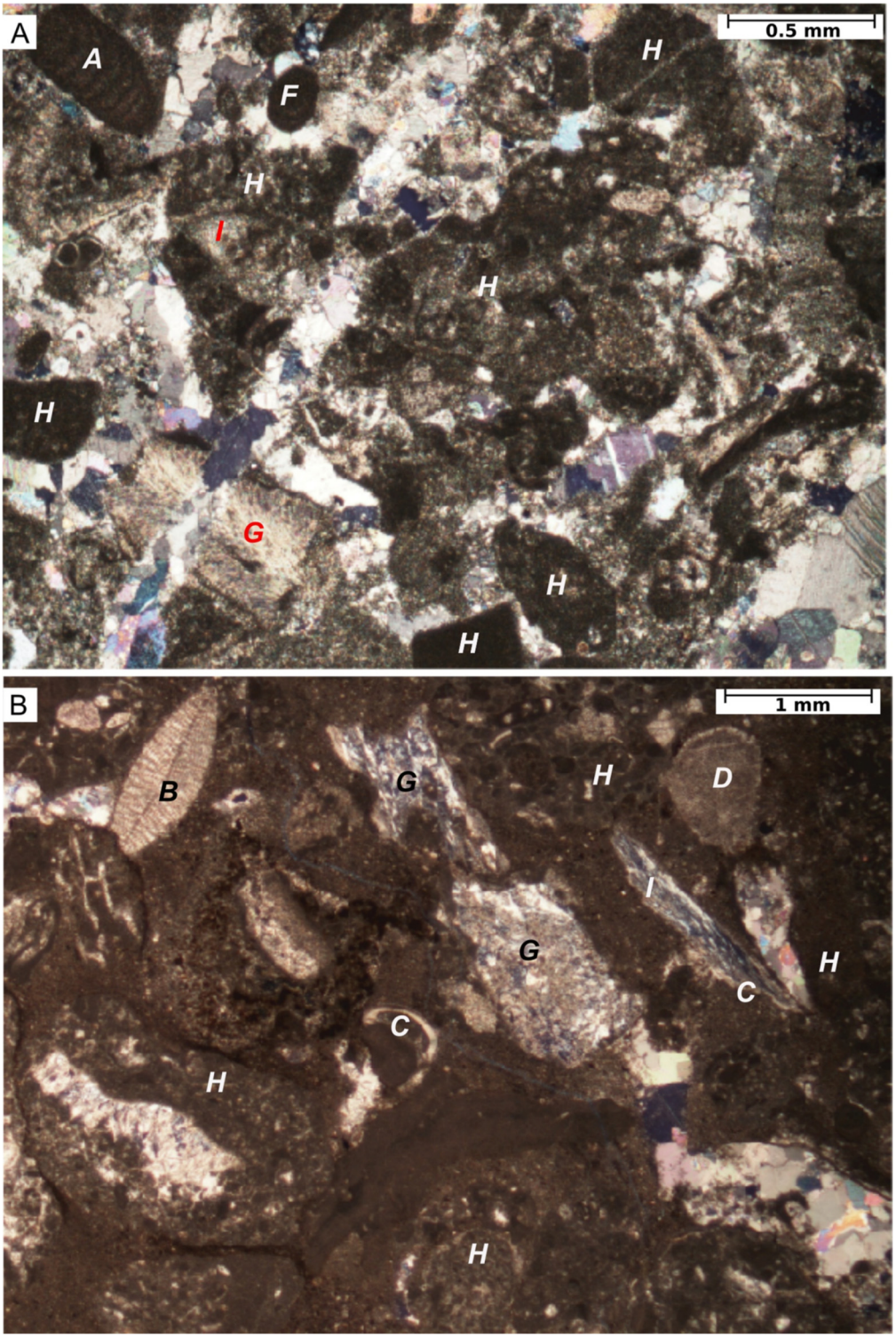

Figure 2. Photomicrographs of carbonate allochems and diagenetic features. Allochems: A–red algae, B–foraminifera, C–mollusk, D–echinoderm, F–peloid, G–bioclast, H–lithic, and I–quartz. Diagenetic features—coarse- and fine-grained calcite cement, silicification, and minor compaction. Scales for parts A and B are 0.5 mm and 1 mm, respectively.

nifera (including benthic discocyclinids and unidentified benthic and planktic foraminifera). Many fossil fragments appear to have been weathered from larger micritic limestone clasts, as suggested by the fragments' micritic texture. To some extent, all fossil fragments in the Toledo sandstones have been affected by recrystallization and cementation.

Toledo sandstones contain a variety of igneous rock fragments, which include finely crystalline igneous clasts, some of which contain small crystals of plagioclase and quartz in a fined-grained crystalline groundmass. Coarsely crystalline igneous rock fragments commonly consist of polycrystalline quartz, mica, finely crystalline fragments, and opaque minerals. There are also rare ultramafic and mafic crystalline rock fragments, which could be classified as serpentinite, peridotite, greenstone, or amphibolite.

Quartz grains in Toledo sandstones include monocrystalline, polycrystalline, and sheared/stretched composite quartz. The monocrystalline quartz commonly contains inclusions of plagioclase and unidentifiable inclusions. Rare feldspar grains n the samples include plagioclase, orthoclase, and perthite.

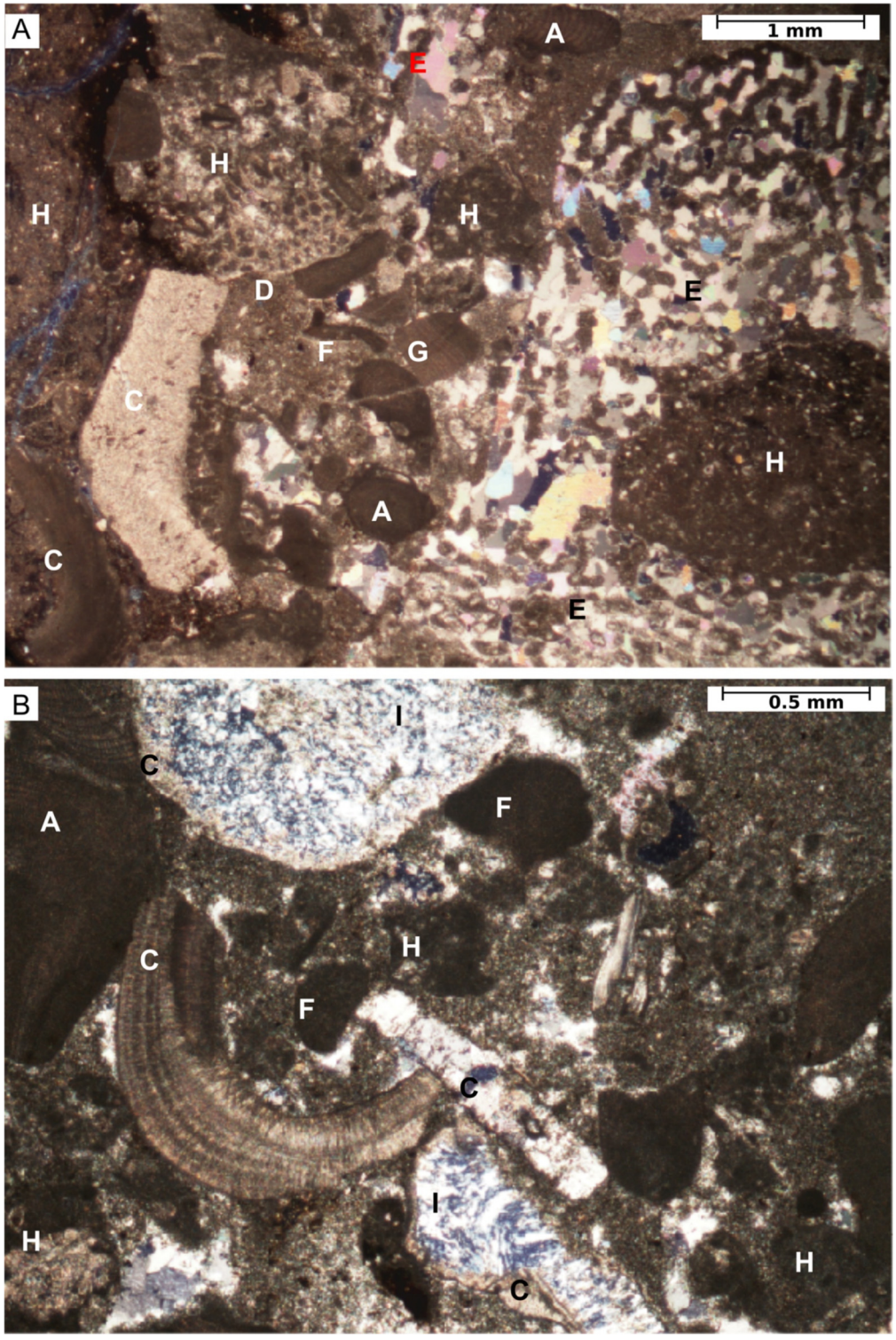

Figure 3. Photomicrographs of carbonate allochems and diagenetic features. Allochems: A–red algae, B–foraminifera, C–mollusk, D–echinoderms, E–coral, F–peloid , G–bioclast, H–lithics, and I–quartz. Diagenetic features—coarse- and fine-grained calcite cement, silicification (represented by presence of chalcedony/chert), and minor compaction. Scales for parts A and B are 1 mm and 0.5 mm, respectively.

Rare occurrences of zoning in feldspar are also observed. Accessory grains in the sandstones include mica and organic detritus.

In the Toledo sandstones, a high percent of lithic fragments combined with textural features, such as poor to moderate sorting and angular to rounded grains indicate transportation over short distances from diverse lithic sources in the near vicinity (Boggs, 2012). Further, the presence of angular feldspars is indicative of a high-relief source area that experienced rapid erosion (Boggs, 2012).

Clastic Provenance

Two ternary diagrams of Dickinson (1985) were used for this study: QFL and QmFLt ternary plots (Figs. 8 and 9). The QFL diagram emphasizes grain stability and maturity and thus focuses on weathering, provenance relief, transport, and source rock based on total quartz, feldspar and lithics (Dickinson and Suczek, 1979; Dickinson, 1985). On Figure 8, the data largely plot as recycled orogen with some samples falling in the magmatic arc (undissected and transitional arc) provenance fields. The

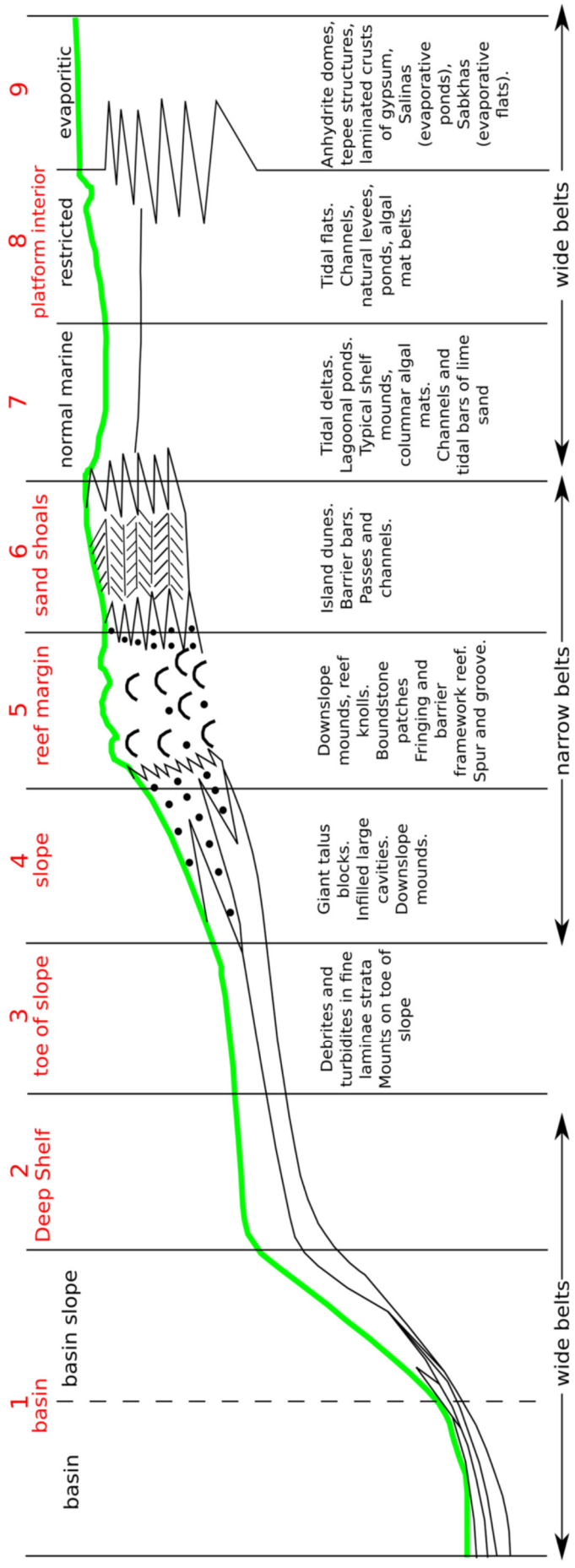

Figure 4. Schematic cross-sectional description of Schlager's (2005) standard "T facies" (tropical carbonate facies) with name and number of facies labeled above each (modified after Schlager, 2005). The cross section shows typical facies geometry and notes the fine-scale features characteristic of each facies.

emphasis of QmFLt ternary diagram is on source rock where all unstable lithic fragments (Qp, Lv, and Ls) are plotted together as Lt (see also Table 3). On Figure 9, all the samples plot within the recycled orogen field between transitional and lithic orogen. Orogenic recycling occurs in several tectonic settings where rocks are deformed, uplifted and eroded, for example, subduction complexes, backarc thrust belts, and suture belts.

In this instance, the Belize Basin, which is the location for Toledo recycling, is the eastern extension of the Chapayal Basin or Southern Petén Basin in Guatemala, located south of the La Libertad Arch and Maya Mountains (Figs. 1 and 10; Vinson, 1962). The basin also lies on the northern edge of the folded and faulted mountains (mainly composed of limestone) and a metamorphic and volcanic complex that Vinson [1962], called a geanticline, or an anticline of regional extent. The collision of the North American and Caribbean plates created both the Polochic and Motagua fault systems (Fig. 1), two parallel fault systems that pass just south of Belize near the southern limit of the Belize Basin (Ramanathan and Garcia, 1991; Leroy et al., 2000). During this time, an accretionary complex developed onshore Guatemala, called the El Tambor complex (Case, 1980). The El Tambor complex includes a suite of ultramafic to mafic rocks (including serpentinite, serpentinite mélange, peridotite, mylonized gabbro and diorites, greenstones, and amphibolites), low grade metamorphic sediments, and metamorphosed pillow lavas and chert (Fig. 10) (Case, 1980). The El Tambor complex is the suggested source of the ultramafic and mafic grains present in the Toledo sandstones.

Quartz grains show a clear dominance of monocrystalline over polycrystalline quartz, suggesting sediments were derived from a granitic source. Movement on the parallel Polochic and Motagua fault zones has exposed igneous rock and metasediments to erosion and recycling (Case, 1980). The El Tambor igneous rocks are largely felsic and include rhyolites, two mica granites, and granite porphyries. Based on its lithic content, the El Tambor accretionary complex is suggested as an important contributing source for the Toledo formation sandstones.

In some parts of the formation, the Toledo contains a high volume percent of carbonate grains. This type of grain was not considered in the generic provenance determination by Dickinson (1985). However, their occurrence in the Toledo is clearly important. Extensive outcrops of Cretaceous carbonate units occur in Guatemala and adjacent Belize, and the folded and faulted limestone mountains of Guatemala are located just south of the Belize basin along the Polochic and Motagua fault zones. This proximity suggests that these areas are very likely contributing sources of the carbonate grains for the Toledo formation.

DIAGENESIS

Compaction, cementation, micritization, and silicification are the main processes of diagenesis in the Toledo formation. The three major porosity types in the Toledo formation are: inter-particle, intra-particle, and fracture porosity. Compaction and cementation have occluded much of the inter-particle primary porosity, and intra-particle porosity has been affected by cementation (Figs. 2–3, 6–7, and 11–12).

Three generations of calcite cement are identified in the samples. The first is a rim of fine-grained, sparry calcite crystals

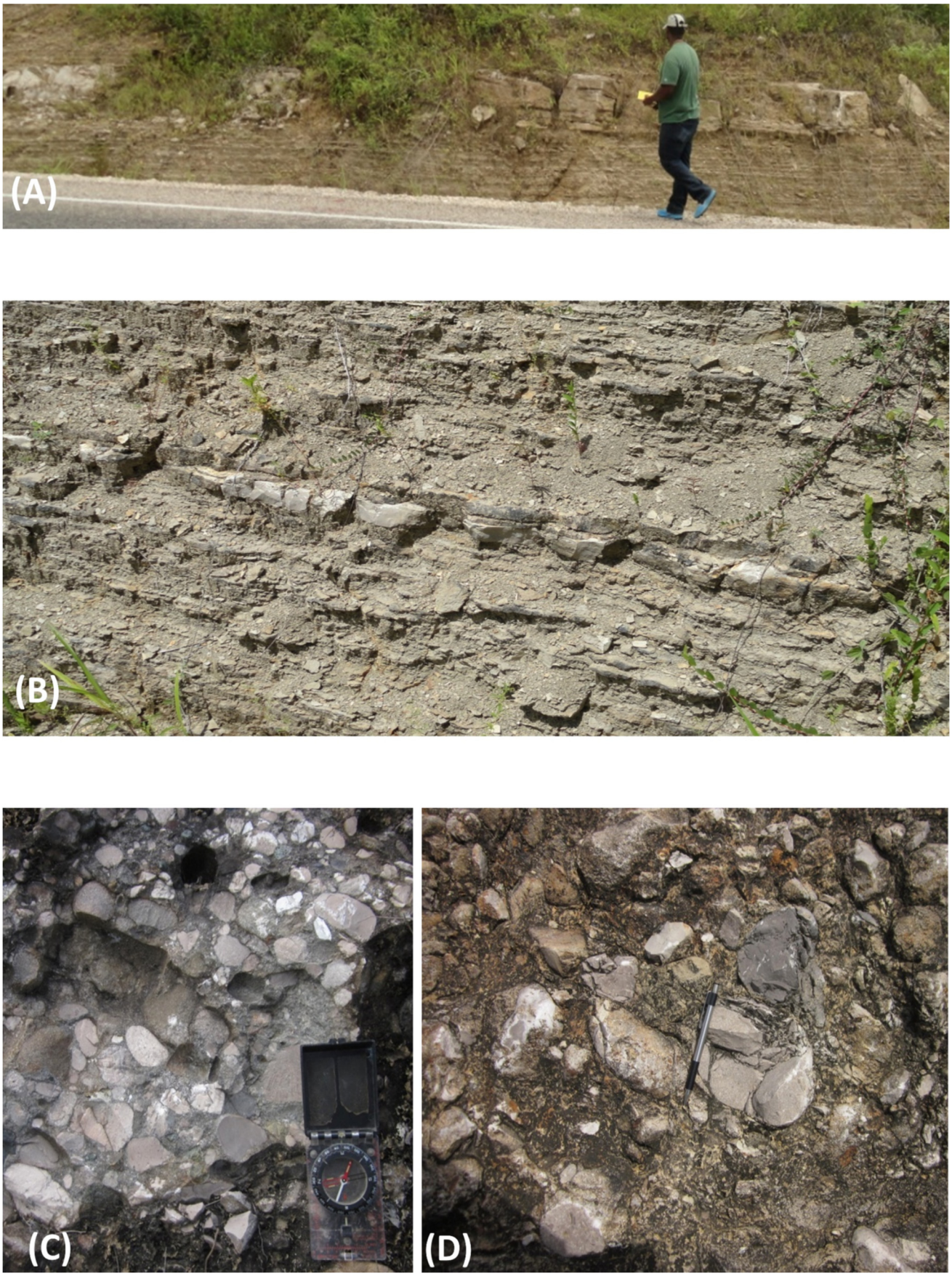

Figure 5. Outcrop photographs of two Toledo carbonate facies, as described in the text. (A) Relatively continuous, tan to buff wackestone bed (0.3 m thick) within a sequence of fine clastic beds. Mile 14 Highway. (B) Tan wackestone and packstone beds intercalated with fine clastic layers. Mile 14 Highway. (C) Large slab of carbonate breccia. Brunton compass scale. Mile 14 Highway. (D) Outcrop showing common texture in carbonate breccia. Pen (5 cm) for scale. Mile 14 Highway.

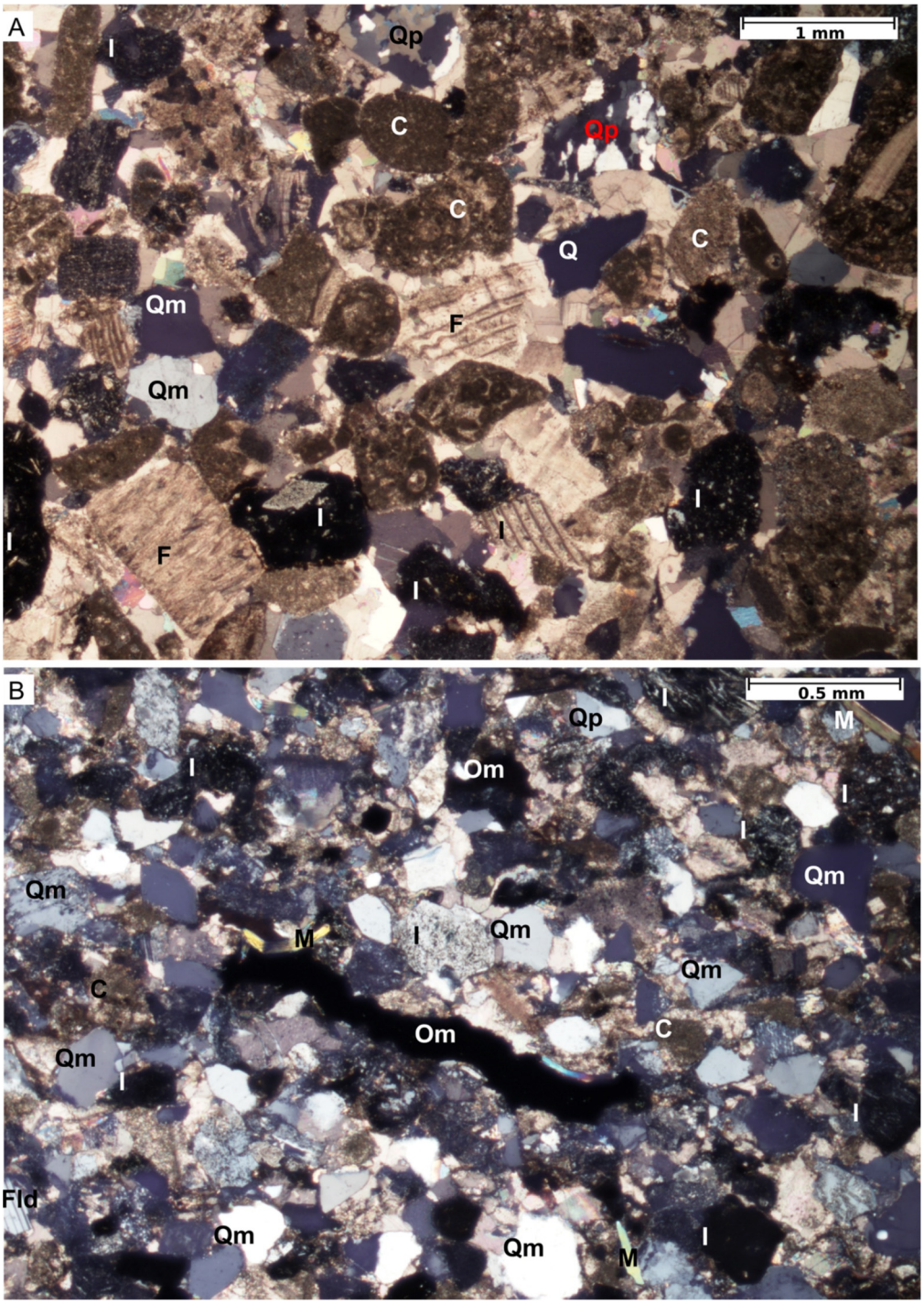

Figure 6. Photomicrographs of Toledo sandstones showing igneous grains (I), carbonate grains (reworked, micritized [C] and fossil fragments [F]), quartz (polycrystalline, Qp, and monocrystalline, Qm), feldspar (Fld), organic matter (Om), and mica (M). Flexible deformation is shown in the mica grains (owing to compaction). Scale for parts A and B are 1 mm and 0.5 mm, respectively.

with a fibrous habit coating intra-particle pore spaces. The second is fine-grained sparry calcite cement occluding intra- and inter-particle pore spaces and fracture pores. The third is medium to coarse blocky/equant cement that also occludes intra- and inter-particle pore spaces and fracture pores. There is an overall increase in crystal size from the pore margins to the center (i.e., a drusy mosaic). The patterns of cementation are consistent with marine phreatic (fibrous calcite cement) and meteoric phreatic zones (equant calcite cement and drusy mosaic; Longman, 1980). Secondary quartz as overgrowths on detrital grains (monocrystalline quartz) is rare (Fig. 11). These overgrowths may represent pre-existing silica cement.

Silicification is relatively rare throughout the samples but is clear where the silica replacement process has manifested itself as an inter-particle pore-filling variety of microquartz, possibly chert. Silica diagenesis also selectively occurs in rare skeletal grains, destroying the grain's original fabric as the carbonate was replaced by finely crystalline silica.

The readily observable effects of physical compaction are minor, and are largely manifested as micro-fractures, flexible-grain deformation, and the effect of concavo-convex and elongated grain contacts. Micro-fractures in the samples apparently only affect particular grains, including carbonate and igneous rock clasts and micas. Micas alone exhibit flexible-grain deformation.

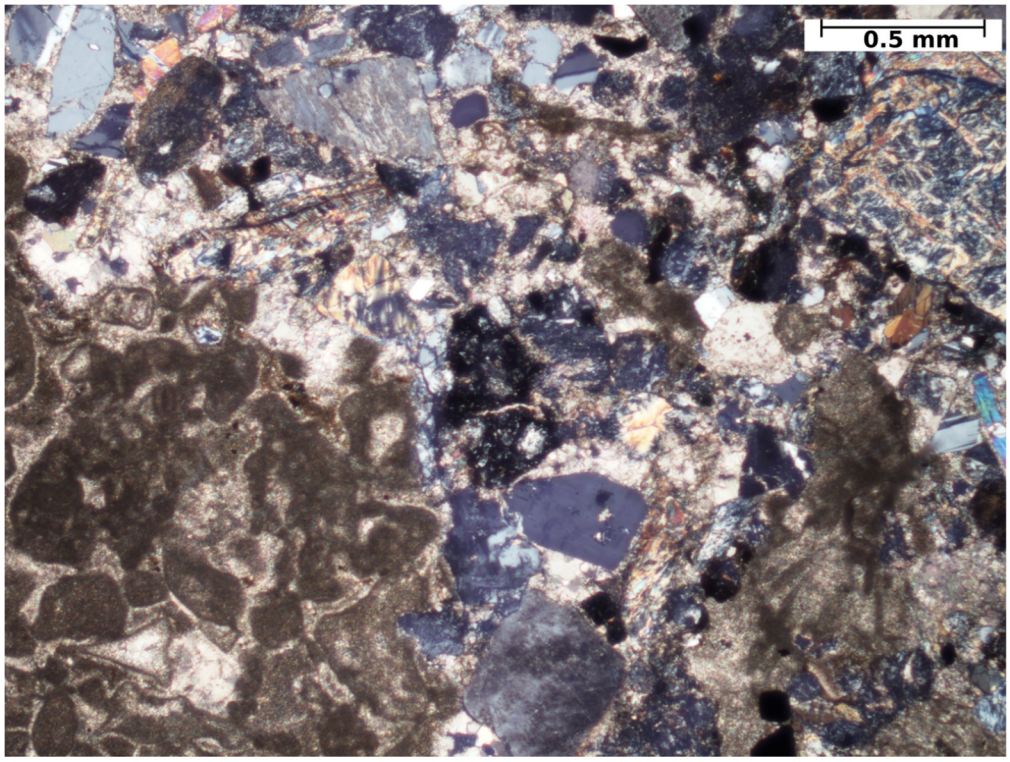

Figure 7. Photomicrograph of Toledo sandstones showing diagenetic features: fine- and coarse-grained calcite cement, minor silicification in carbonate grain in the bottom left, fracture in lithic and quartz grains (compaction), and concavo-convex and long contacts between lithic fragments. Scale on figure is 0.5 mm.

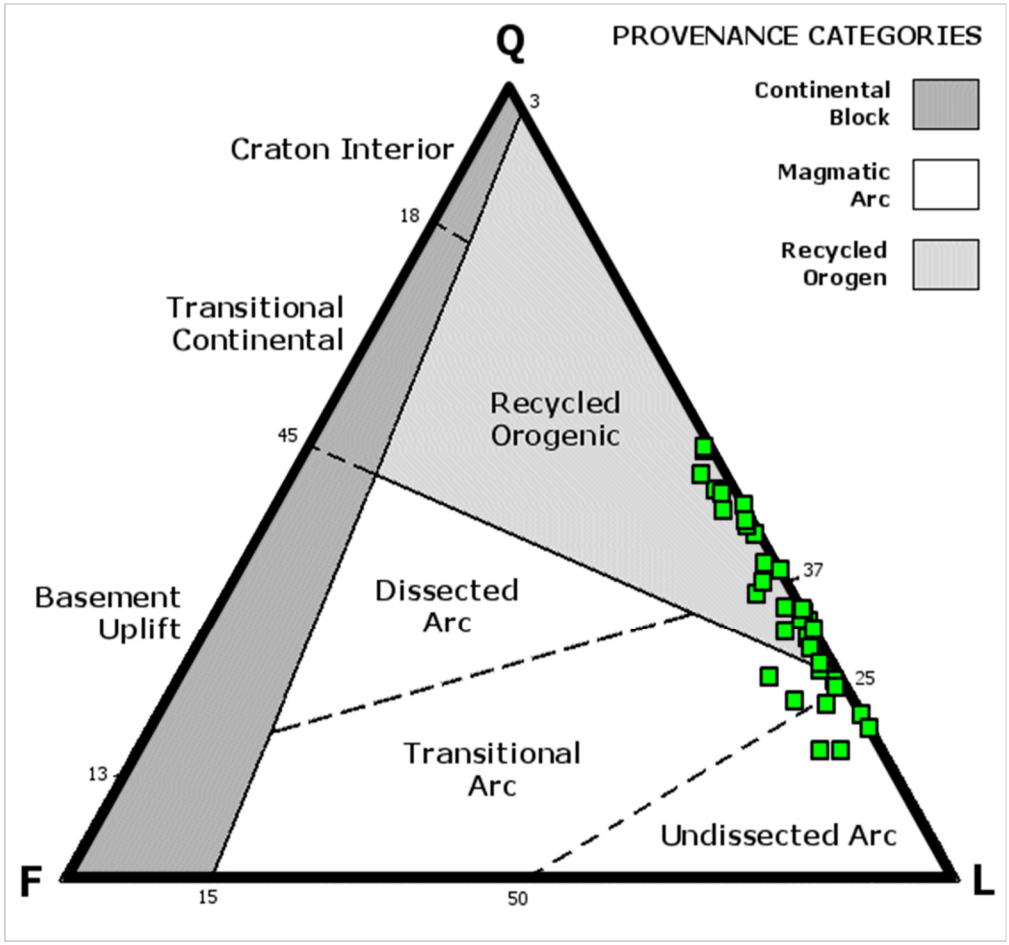

Figure 8. A QFL plot of the Toledo formation sandstones in this study. Plot format follows that of Dickinson (1985).

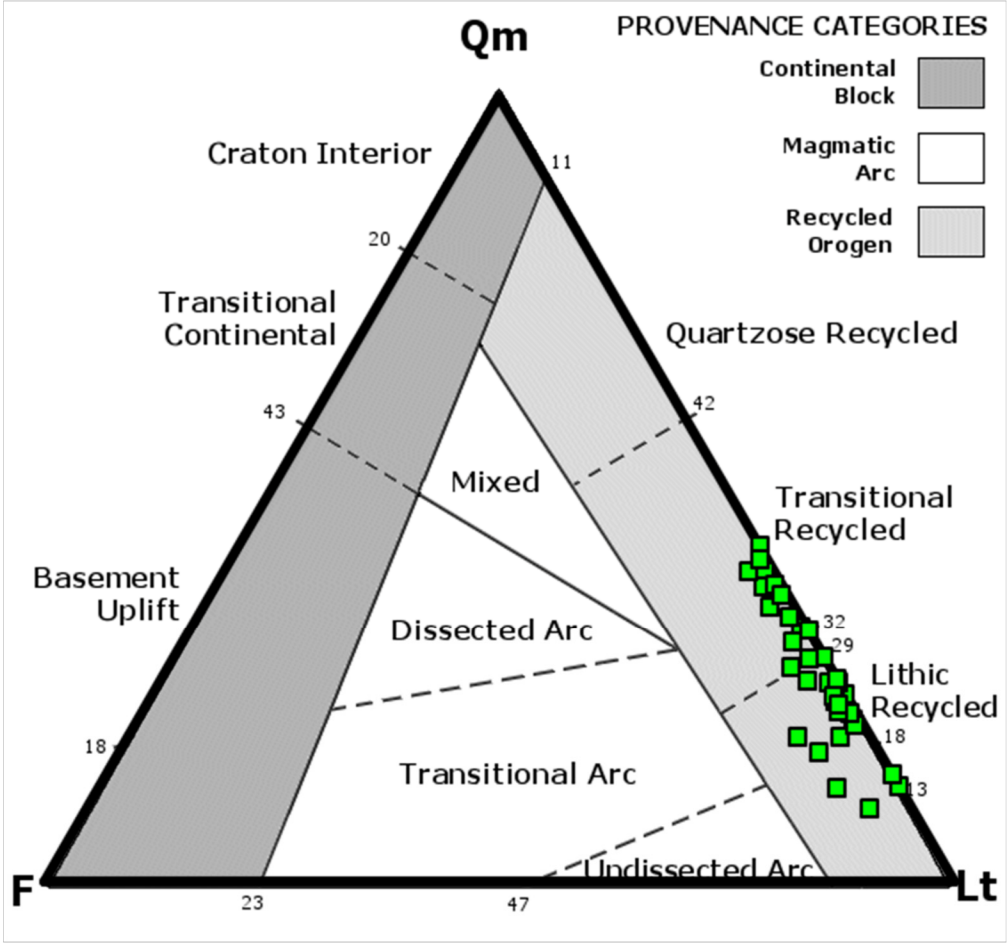

Figure 9. A QmFLt plot of the Toledo formation sandstones in this study. Plot format follows that of Dickinson (1985).

Concavo-convex and elongated contacts occur between lithic fragments (igneous and sedimentary), and quartz and feldspar grains (Figs. 11 and 12).

ECONOMIC POTENTIAL

Reservoir development is largely dependent on the original sandstone composition, which in turn influenced by sediment source and tectonic history. The Toledo sandstones are texturally submature and mineralogically immature. Texturally immature sandstones typically display less porosity and permeability, thus decreasing the reservoir potential. Reservoir quality is also affected by subsequent diagenesis of the sandstones. Porosity occlusion points to the poor reservoir rock potential of the sandstones whether for oil and gas or groundwater resources. However, porosity occlusion coupled with thick interbeds of mudstone and siltstone and the formation's extensive thickness, suggests that the Toledo may serve as a good seal for Cretaceous reservoirs. The sandstones also have stratigraphic trapping potential as a diagenetic barrier due to porosity occlusion.

CONCLUSIONS

Within the Toledo formation, there is a dominance of non-skeletal grains, as well as skeletal fragments that are largely composed of restricted marine assemblages such as red algae, gastropods, and foraminifera. The carbonates, both wackestone-packstone and carbonate breccias are interpreted to be deposited in a slope setting, which is consistent with the facies model of Schlager (2005).

The Toledo sandstones are classified as lithic arenites that are texturally submature (dominated by angular to subrounded grains that are poorly to moderately sorted). Compositionally, they are immature due to the dominance of unstable lithic fragments. Diagenetic features include carbonate cement characteristic of marine and meteoric phreatic zones. These features, coupled with the submature nature of the sandstones limits the potential of the sandstones as reservoirs for hydrocarbon or groundwater resources. However, the formation could serve as a seal for Cretaceous reservoirs. The composition of the Toledo sandstones indicates that the provenance area is a recycled orogen related to the collision of the North American and Caribbean tectonic plates.

ACKNOWLEDGMENTS

The authors are grateful to the Big Creek Group of Companies for their partial support of this work and their interest in seeking a better understanding of the geological history of Belize.

REFERENCES CITED

Bhatia, M. R., 1983, Plate tectonics and geochemical composition of sandstone: Journal of Geology, v. 91, p. 611–627, <https://doi.org/10.1086/628815>.

Boggs, S., Jr., 2012, Principles of sedimentology and stratigraphy, 5th ed.: Pearson Prentice Hall, New York, 688 p.

Bryson, R. S., 1975, Stratigraphy problems of northern Belize: Anschutz Overseas Corporation, Denver, Colorado, 22 p.

Case, J. E., 1980, Crustal setting of mafic and ultramafic rocks and associated ore deposits of the Caribbean region: U.S. Geological Survey Open-File Report 80–304, 99 p.

Dickinson, W. R., 1985, Interpreting provenance relations from detrital modes of sandstones, *in* G. G. Zuffa, ed., Provenance of

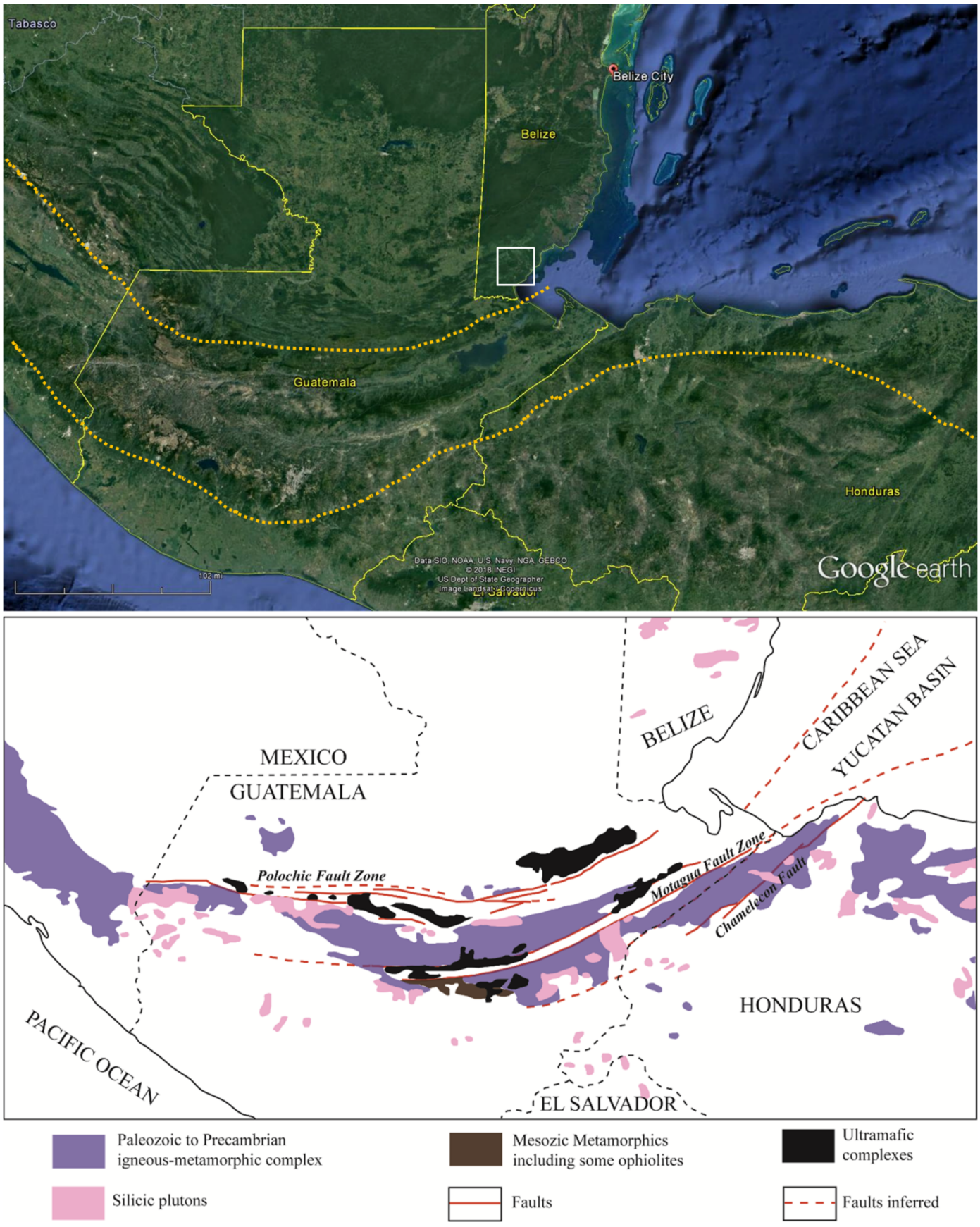

Figure 10. Upper part—Google Earth® image of Belize area with white box showing area of map in lower part of Figure 1 (i.e., the study area). Dotted lines show limits of the El Tambor accretionary complex as shown in the lower part. Lower part—Map showing the geological location of the El Tambor accretionary complex of Guatemala (modified after Case, 1980).

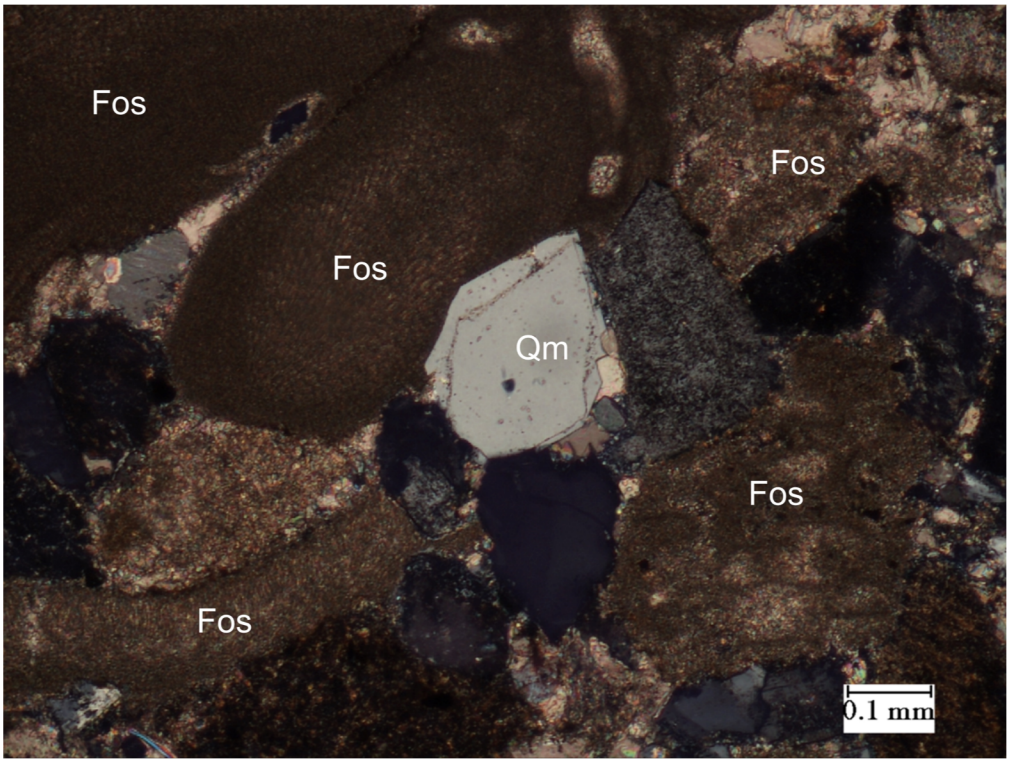

Figure 11. Photomicrograph of Toledo sandstone showing diagenetic features: quartz overgrowth and long contact between quartz grain (monocrystalline, Qm) and fossil fragment (Fos). Scale is 0.1 mm.

arenites: Springer-Verlag, Berlin, Germany, p. 333–361, <https://doi.org/10.1007/978-94-017-2809-6_15>.

Dickinson, W. R., L. S. Beard, G. R. Brakenridge, J. L. Erjavec, R. C. Ferguson, K. F. Inman, R. A. Knepp, F. A. Lindberg, and P. T. Ryberg, 1983, Provenance of North American Phanerozoic sandstones in relation to tectonic setting: Geological Society of America Bulletin, v. 93, p. 222–235, <https://doi.org/10.1130/0016-7606(1983)94%3C222:PONAPS%3E2.0.CO;2>.

Dickinson, W. R., and C. A. Suczek, 1979, Plate tectonics and sandstone compositions: American Association of Petroleum Geologists Bulletin, v. 63, p. 2164–2182, <https://doi.org/10.1306/2F9188FB-16CE-11D7-8645000102C1865D>.

Donnelly, T. W., D. Beets, M. J. Carr, T. Jackson, G. Klaver, J. Lewis, R. Maury, H. Schellenkens, A. L. Smith, G. Wadge and D. Westercamp, 1990, History and tectonic setting of Caribbean magmatism, *in* G. Dengo and J. E. Case, eds., The geology of North America, v. H: The Caribbean region: Geological Society of America, Boulder, Colorado, p. 339–374, <https://doi.org/10.1130/DNAG-GNA-H.339>.

Fisher, J. D., and D. T. King, Jr., 2015, Stratigraphy of the Toledo formation, Belize Basin, southern Belize: Gulf Coast Association of Geological Societies Transactions, v. 65, p. 107–123.

Fisher, J. D., and D. T. King, Jr., 2016, Lower Cenozoic fan deposits in southern Belize: Gulf Coast Association of Geological Societies Transactions, v. 66, p. 181–195.

JMicroVision, 2018, JMicroVision software, <https://www.download.hr/software-jmicrovision.html>.

Kim, Y., R. W. Clayton, and C. Keppie, 2011, Evidence of a collision between the Yucatán block and Mexico during Miocene: Geophysical Journal International, v. 187, p. 989–1000.

King, D. T., Jr., K. O. Pope, and L. W. Petruny, 2004, Stratigraphy of Belize, north of the 17th parallel: Gulf Coast Association of Geological Societies Transactions, v. 54, p. 289–304.

Leroy, S., A. Mauffret, P. Patriat, and B. Mercier de Lépinay, 2000, An alternative interpretation of the Cayman trough evolution from reidentification of magnetic anomalies: Geophysical Journal International, v. 141, p. 538–557.

Longman, M. W., 1980, Carbonate diagenetic textures from near surface diagenetic environments: American Association of Petroleum Geologists Bulletin, v. 64, p. 461–487, <https://doi.org/10.1306/2F918A63-16CE-11D7-8645000102C1865D>.

Purdy, E. G., E. Gischler, and A. J. Lomando, 2003, The Belize margin revisited, 2—Origin of Holocene antecedent topography: International Journal of Earth Sciences, v. 92, p. 552–572, <https://doi.org/10.1007/s00531-003-0325-z>.

Ramanthan, R. and E. Garcia, 1991, Cretaceous paleogeography, foraminiferal biostratigraphy, and paleoecology of Belize basin: Transactions of the 2nd Geological Conference of the Geological Society of Trinidad and Tobago, Port of Spain, p. 203–211.

Roster, B. P., and R. J. Korsch, 1986, Determination of tectonic setting of sandstone-mudstone suites using SiO_2 content and K_2O/Na_2O ratio: Journal of Geology v. 94, p. 635–650, <https://doi.org/10.1086/629071>.

Schlager, W., 2005, Carbonate sedimentology and sequence stratigraphy: Society of Economic Paleontologists and Mineralogists (Society for Sedimentary Geology) Concepts in Sedimentology and Paleontology 8, Tulsa, Oklahoma, 206 p., <https://doi.org/10.2110/csp.05.08>.

Vinson, G. L., 1962, Upper Cretaceous and Tertiary stratigraphy of Guatemala: American Association of Petroleum Geologists Bulletin, v. 62, p. 425–456.

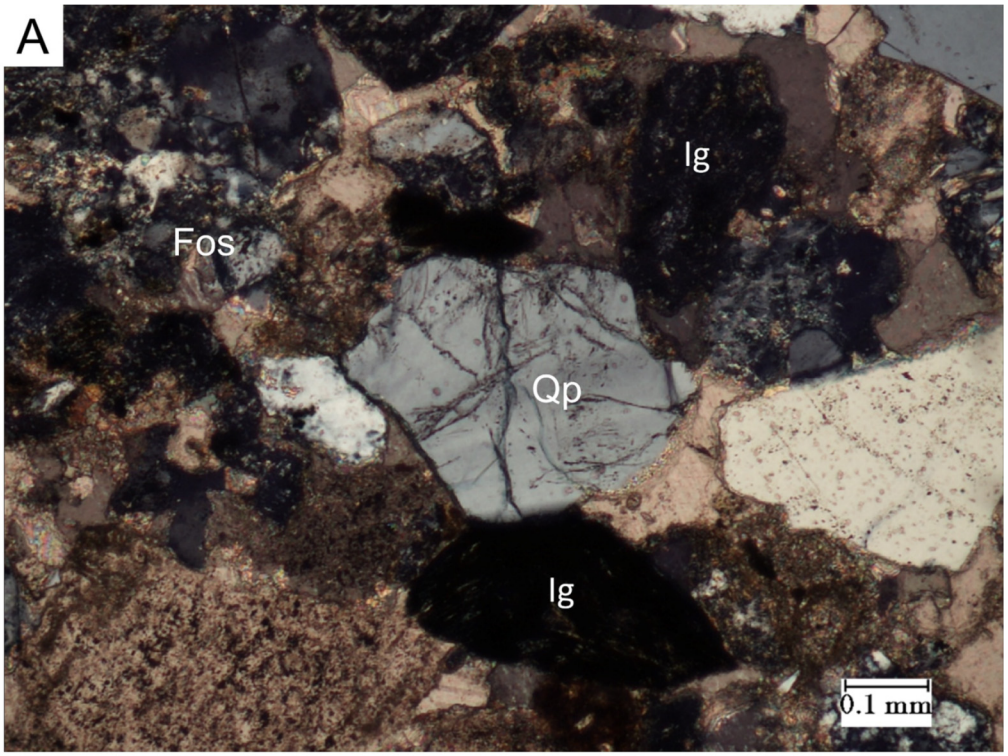

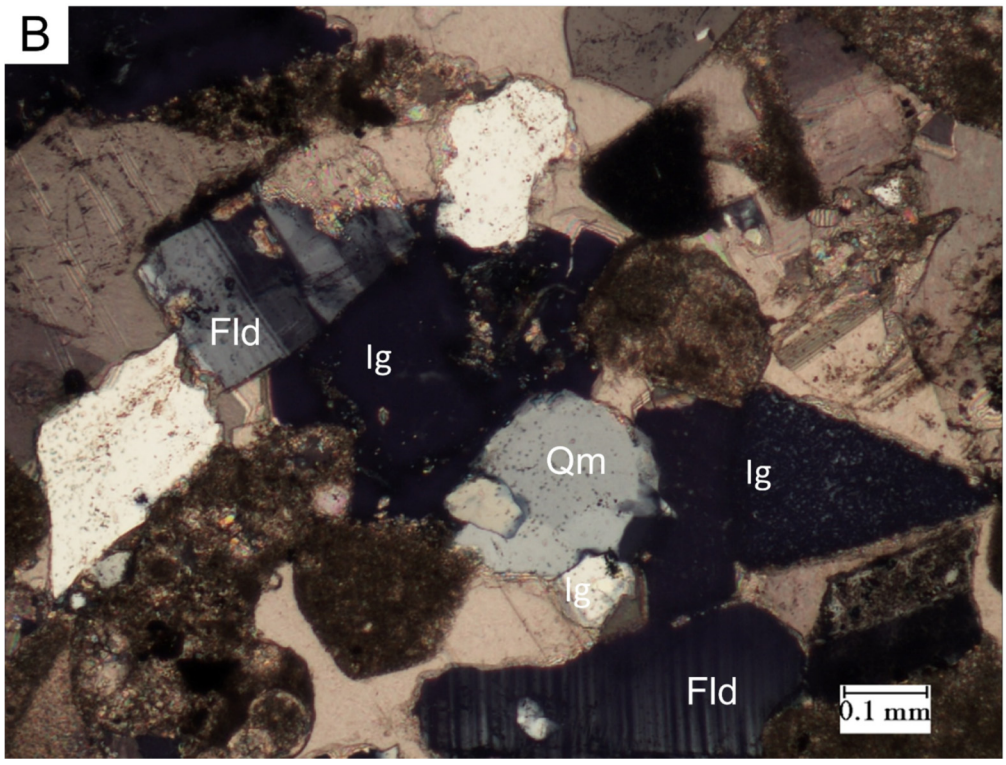

Figure 12. Photomicrographs of Toledo sandstones showing diagenetic features. (A) Physical compaction between quartz and igneous lithic fragment as concavo-convex contacts. (B) Physical compaction between feldspar (Fld), igneous lithic fragment (lg), fossil (Fos), and quartz grain (polycrystalline, Qp, and monocrystalline, Qm). Scale of both A and B is 0.1 mm.